



A linear B-spline interpolation/Galerkin finite element method for the two-dimensional Riesz space distributed-order diffusion-wave equation with error analysis

M. H. Derakhshan¹, H. R. Marasi^{1,2,a}, Pushpendra Kumar^{3,4,5}

¹ Department of Applied Mathematics, Faculty of Mathematics, Statistics and Computer Science, University of Tabriz, Tabriz, Iran

² Research Department of Computational Algorithms and Mathematical Models, University of Tabriz, Tabriz, Iran

³ Department of Mathematics, Mathematics Research Center, Near East University TRNC, Mersin 10, Turkey

⁴ Faculty of Engineering and Natural Sciences, Istanbul Okan University, Istanbul, Turkey

⁵ Institute for the Future of Knowledge, University of Johannesburg, Auckland Park 2006, PO Box 524, Johannesburg, South Africa

Received: 28 April 2023 / Accepted: 31 January 2024

© The Author(s), under exclusive licence to Società Italiana di Fisica and Springer-Verlag GmbH Germany, part of Springer Nature 2024

Abstract This paper focuses on the distributed-order time-fractional diffusion-wave equations with the Riesz space fractional derivatives. A combined method based on the midpoint quadrature rule, linear B-spline interpolation, and the Galerkin finite element method is proposed to obtain the approximate solution. Two steps are used to calculate the approximate solution to this type of equation. The first step approximates the temporal direction by combining a midpoint quadrature rule and linear B-spline interpolation. In the second step, a Galerkin finite element method in the space direction is applied to compute a full-discrete method. Furthermore, the error estimate has been displayed to demonstrate unconditional stability and convergence. Finally, two numerical examples are reported to show the simplicity and efficiency of the proposed method.

1 Introduction

Fractional calculus has been considered for many physical phenomena in science and engineering due to its attractive concepts and topics. For example, mathematical models in finance [28], mathematical model of atmospheric dynamics of CO_2 gas [27], environmental phenomena [12–14, 38], physical aspects [3, 26, 29, 44], engineering models in optimal control [6] and their references. The fractional differential equations in fractional calculus play a major and important role in simulating and modeling many practical and natural phenomena [15]. The importance and key advantages of differential equations in fractional calculus have been reported in the electrical properties of real materials, the study of rheological properties, and various fields of mathematical and physical sciences such as probability and electrical networks [19, 23, 40, 42]. Recently, several numerical methods have been proposed to simulate various types of fractional-order systems [30, 37, 41].

For the first time, the study and analysis of distributed-order differential equations was done by Caputo [11] to study stress–strain relations in unelastic media. Later, detailed research on the properties of distributed-order operators and on the properties and solution methods of distributed-order differential equations was made in [8, 33]. The study of fractional differential equations was done by Gorenflo et al. [20], in which they investigated the solutions using a combination of the Fourier-Laplace transform and the interpolation method. In [31], the authors studied a method based on the eigenfunctions expansion method in combination with the Laplace transform to discuss the analytical solutions of distributed-order differential equations. Calculating exact solutions for many differential equations of distributed order is not easy. For this reason, it becomes important and valuable to check and study numerical solutions using numerical techniques. Here we describe some of the numerical techniques that are used to calculate the approximate solutions to such types of equations. For example, compact difference method [47], hybrid functions [34], finite element method [5], Galerkin finite element method [32], difference method [21], shifted Grünwald formula [49], fractional centered difference formula [48], orthonormal piecewise Jacobi functions [24], Müntz-Legendre polynomials [43], Laplace and Hankel transforms [1], fast high-order compact difference method [39], an alternating direction implicit Galerkin finite element method [46], Tau method and fractional-order Gegenbauer wavelets [35], operational matrices based on the fractional Chelyshkov wavelets [36], finite difference method and integral transforms [2], Laplace-type integrals, the Gauss-Laguerre quadrature [4] and the known L1 method [25]. The interest and attraction of distributed-order fractional operators of distributive order go back to the 1990s and early 2000s. The interest in this topic went beyond the mathematical community and started percolating into several branches of engineering and physics. For sufficient information in this field, we estimate that more than 200 articles in various fields involving distributive order fractional

^a e-mail: marasi@tabrizu.ac.ir (corresponding author)

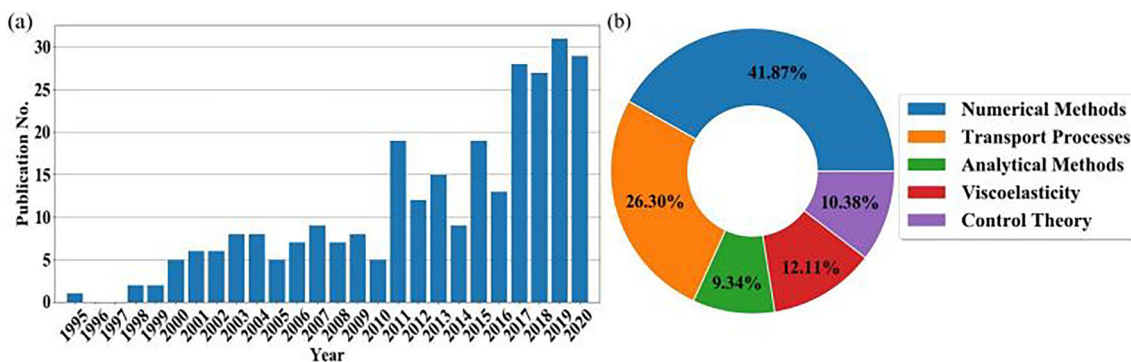


Fig. 1 a Histogram chart of scientific publications per year starting from 1995. b Pie chart

operators have been published. This approximation contains both journal and conference publications spanning a diversity of areas, including, but not limited to, theoretical and applied mathematics and analytical and control theory.

A complete survey of the scientific studies produced in different fields of distributive order as a histogram chart and Pie chart is shown in Fig. 1. This Fig. 1 which is taken from reference [17], is intended to provide the reader with a road map to understand the early development of distributed-order fractional calculus, the progressive evolution, and its application to the modeling of complex real-world problems. To date, we estimate that a total of approximately 300 papers have been published in the general area of distributed-order fractional calculus. This estimate includes both journal and conference publications spanning a variety of fields, including, but not limited to, theoretical and applied mathematics, analytical and numerical methods, viscoelasticity, and control theory. The fractional operators of distributive order can be expressed as a parallel distribution of derivatives of either integer or fractional orders. These fractional operators can be used for modeling physical systems, where reactions are determined by a superposition of different processes operating in parallel and individually studied by either operators of fractional or integer orders [33].

In this paper, we study the following distributed-order time-fractional diffusion-wave equations with the Riesz space fractional derivatives:

$$\int_0^1 b(\beta)^C D_t^\beta w(x, y, t) d\beta = \frac{1}{\Gamma(\mu - 1)} \int_0^t (t - \tau)^{\mu-2} e^{-\omega(t-\tau)} \mathbf{A}_x \frac{\partial^\eta w(x, y, \tau)}{\partial |x|^\eta} d\tau + \frac{1}{\Gamma(\mu - 1)} \int_0^t (t - \tau)^{\mu-2} e^{-\omega(t-\tau)} \mathbf{A}_y \frac{\partial^\nu w(x, y, \tau)}{\partial |y|^\nu} d\tau + g(\mathbf{x}, t), \tag{1.1}$$

in which $\beta \in (0, 1]$, $1 < \mu$, $\eta, \nu \leq 2$, $\omega \geq 0$, under the following initial and boundary conditions:

$$\begin{aligned} w(x, y, 0) &= \psi(x, y), \quad (x, y) \in \Gamma, \\ w(x, y, t) &= 0, \quad (x, y) \in \partial\Gamma, \quad t \in (0, T), \end{aligned} \tag{1.2}$$

where the symbol $b(\beta)$ is the non-negative weight function, and $\mathbf{A}_x, \mathbf{A}_y$ are the positive constants. Here ${}^C D_t^\beta$ shows the Caputo fractional operator of order α , $\frac{\partial^\eta}{\partial |x|^\eta}$ is the Riesz fractional operator in spatial direction. Here, we define the Riesz fractional operator of order η as follows [18]:

$$\begin{aligned} \frac{\partial^\eta w(x, y, t)}{\partial |x|^\eta} &= -\frac{1}{\cos(\frac{\pi\eta}{2})} ({}_a^{RL} D_x^\eta w(x, y, t) + {}_x^{RL} D_b^\eta w(x, y, t)), \\ \frac{\partial^\nu w(x, y, t)}{\partial |y|^\nu} &= -\frac{1}{\cos(\frac{\pi\nu}{2})} ({}_c^{RL} D_y^\nu w(x, y, t) + {}_y^{RL} D_d^\nu w(x, y, t)), \end{aligned}$$

where ${}_a^{RL} D_x^\eta, {}_x^{RL} D_b^\eta, {}_c^{RL} D_y^\nu$ and ${}_y^{RL} D_d^\nu$ are the Riemann-Liouville operators which are defined by the following formulas [42]:

$$\begin{aligned} {}_a^{RL} D_x^\eta w(x, y, t) &= \frac{d^2}{dx^2} (I_{a^+}^{2-\eta} w(x, y, t)), \quad {}_x^{RL} D_b^\eta w(x, y, t) = \frac{d^2}{dx^2} (I_{b^-}^{2-\eta} w(x, y, t)), \\ {}_c^{RL} D_y^\nu w(x, y, t) &= \frac{d^2}{dy^2} (I_{c^+}^{2-\nu} w(x, y, t)), \quad {}_y^{RL} D_d^\nu w(x, y, t) = \frac{d^2}{dy^2} (I_{d^-}^{2-\nu} w(x, y, t)), \end{aligned}$$

in which $I_{a^+}^\eta$ and $I_{b^-}^\eta$ are the Riemann-Liouville fractional integrals stated in [42].

In this article, a combined method is used to obtain the approximate solutions of equation (1.1). In the first step, the midpoint quadrature rule and linear B-spline interpolation are used to discretize the integral part of the distributional order. In the second step, we use the Galerkin finite element method to discretize the space variable to compute a full plan. As well, in this article, the

convergence and stability analyses for the proposed method are studied. The main purpose and interest of this article is to develop and study a numerical method based on the high-order numerical method to enable approximation and rigorously perform its stability analyses and convergence, which are seldom studied in the current literature. Also, one of the approaches of the numerical method presented in this article refers to the computational time and high accuracy during the execution of the programme.

The remainder of the paper is divided as below. In Sect. 2, we state a discretization for the integral part of distributed order applying midpoint quadrature rule and linear B-spline interpolation. Also, in this section, stability analysis is studied. In Sect. 3, we obtain the full-discrete method based on the Galerkin finite element method and the approximate method described in Sect. 2. Moreover, in this section, the convergence analysis for the full-discrete method is discussed. In Sect. 4, we present two numerical examples to verify the effectiveness of the numerical method. In this section, the effectiveness of the proposed method is shown by drawing a diagram and presenting tables. Finally, in Sect. 5, we state the conclusion section.

2 Discretization for the integral part of distributed order

In this section, we display a numerical method for the discretization of the distributed order integral part in time which is demonstrated in the equation (1.1). For this aim, we consider $t_n = n\Delta t$, $\Delta t = \frac{T}{N}$, $N \in \mathbb{N}$ for $n = 0, 1, \dots, N$. To calculate and obtain an approximation for the distribution order integral part, we first find an approximation for the Caputo fractional operator of order β , and then we compute an approximation for the distribution order integral part applying composite midpoint quadrature formula. Then

$${}^C D_{t_n}^\beta w(x, y, t) = \frac{1}{\Gamma(1-\beta)} \int_0^{t_n} (t_n - \tau)^{-\beta} \frac{\partial w(x, y, \tau)}{\partial \tau} d\tau. \tag{2.1}$$

To obtain an approximation for Eq. (2.1), we use linear B-spline to approximate the first-order derivative, then the linear B-spline at point t_l for $l = 0, 1, \dots, n$ is displayed as follows:

$$\begin{aligned} \frac{\partial w(x, y, t)}{\partial t} = \mathbf{S}_n(x, y, t) &= \sum_{j=0}^{n-1} \mathbf{S}_j(x, y, t) = \sum_{j=0}^{n-1} \left[\frac{t - t_{j+1}}{t_j - t_{j+1}} \frac{\partial w(x, y, t_j)}{\partial t} + \frac{t - t_j}{t_{j+1} - t_j} \frac{\partial w(x, y, t_{j+1})}{\partial t} \right. \\ &\quad \left. + \frac{(t - t_j)(t - t_{j+1})}{2} \frac{\partial^3 w(x, y, \varrho_j)}{\partial t^3} \right], \varrho_j \in (t_j, t_{j+1}). \end{aligned} \tag{2.2}$$

By substituting the equation (2.2) into (2.1), we get the following formula:

$$\begin{aligned} {}^C D_{t_n}^\beta w(x, y, t) = {}^C D_{t_n}^\beta \mathbf{S}_n(x, y, t) &= \frac{1}{\Gamma(1-\beta)} \sum_{j=0}^{n-1} \left(\int_{t_j}^{t_{j+1}} (t_n - \tau)^{-\beta} \frac{\tau - t_{j+1}}{t_j - t_{j+1}} \frac{\partial w(x, y, t_j)}{\partial \tau} d\tau \right) \\ &\quad + \frac{1}{\Gamma(1-\beta)} \sum_{j=0}^{n-1} \left(\int_{t_j}^{t_{j+1}} (t_n - \tau)^{-\beta} \frac{\tau - t_j}{t_{j+1} - t_j} \frac{\partial w(x, y, t_{j+1})}{\partial \tau} d\tau \right) \\ &\quad + \frac{1}{2\Gamma(1-\beta)} \sum_{j=0}^{n-1} \left(\int_{t_j}^{t_{j+1}} (t_n - \tau)^{-\beta} \frac{\tau - t_j}{\tau - t_{j+1}} \frac{\partial^3 w(x, y, \varrho_j)}{\partial \tau^3} d\tau \right). \end{aligned} \tag{2.3}$$

With a simple calculation, the following formula is obtained:

$${}^C D_{t_n}^\beta w(x, y, t) = \frac{(\Delta t)^{1-\beta}}{\Gamma(3-\beta)} \sum_{j=0}^n \mathbf{a}_{j,n}^\beta \frac{\partial w(x, y, t_j)}{\partial t} + \mathcal{O}((\Delta t)^{3-\beta}), \tag{2.4}$$

in which the coefficients $\mathbf{a}_{j,n}^\beta$ is calculate as follow:

$$\mathbf{a}_{j,n}^\beta = \begin{cases} (n-1)^{2-\beta} - n^{1-\beta}(n-2+\beta), & j=0, \\ (n-j+1)^{2-\beta} - 2(n-j)^{2-\beta} + (n-j-1)^{2-\beta}, & j=1, 2, \dots, n-1, \\ 1 & j=n. \end{cases} \tag{2.5}$$

Now, to estimate the distributed order fractional integral part, we divide the specified interval $[0, 1]$ into m subintervals $[\beta_{i-1}, \beta_i]$, $i = 1, 2, \dots, m$, $m \in \mathbb{N}$. Consider $\zeta_i = \frac{\beta_{i-1} + \beta_i}{2}$. Thus, using the composite midpoint quadrature formula, we get

$$\int_0^1 b(\beta) {}^C D_t^\beta w(x, y, t) d\beta = h \sum_{i=1}^m b(\zeta_i) {}^C D_{t_n}^{\zeta_i} w(x, y, t) + \mathcal{O}(h^2). \tag{2.6}$$

By inserting the right-hand side of Eq. (2.4) into (2.6), we obtain

$$\begin{aligned} \int_0^1 b(\beta)^C D_t^\beta w(x, y, t) d\beta &= h \sum_{i=1}^m b(\zeta_i) \left(\frac{(\Delta t)^{1-\zeta_i}}{\Gamma(3-\zeta_i)} \sum_{j=0}^n \mathbf{a}_{j,n}^{\zeta_i} \frac{\partial w(x, y, t_j)}{\partial t} \right) + \mathcal{O}(h^2) + \mathcal{O}((\Delta t)^{3-\zeta_m}) \\ &= \sum_{j=0}^n \mathbf{b}_{j,n} \frac{\partial w(x, y, t_j)}{\partial t} + \mathcal{O}(h^2) + \mathcal{O}((\Delta t)^{3-\zeta_m}) \\ &= \sum_{j=0}^n \mathbf{b}_{j,n} \frac{\partial w(x, y, t_j)}{\partial t} + \mathcal{O}(h^2 + (\Delta t)^{2+\frac{h}{2}}), \end{aligned} \tag{2.7}$$

in which $\mathbf{b}_{j,n} = h \sum_{i=1}^m b(\zeta_i) \frac{(\Delta t)^{1-\zeta_i}}{\Gamma(3-\zeta_i)} \mathbf{a}_{j,n}^{\zeta_i}$, $h = \frac{1}{m}$ and $\beta_i = ih$.

Lemma 2.1 [9] Assume that $\mu \in (1, 2]$. Then the numerical discrete method for the fractional integral in time is computed by

$$\begin{aligned} I_t^{\mu-1, \gamma} w(x, y, t) \Big|_{t=t_n} &= \frac{1}{\Gamma(\mu-1)} \int_0^{t_n} (t_n - \tau)^{\mu-2} e^{-\gamma(t_n-\tau)} w(x, y, \tau) d\tau \\ &= (\Delta t)^{\mu-1} \sum_{l=0}^n \xi_l^{\mu-1} w(x, y, t_{n-l}) + \mathcal{O}((\Delta t)^2), \quad \gamma \geq 0, \end{aligned} \tag{2.8}$$

where the coefficients $\xi_l^{\mu-1}$ is defined by

$$\xi_l^{\mu-1} = \left(\frac{3}{2}\right)^{\mu-1} e^{-\gamma l \Delta t} \sum_{q=0}^l (z_q z_{l-q})^{1-\mu} 3^{-q}. \tag{2.9}$$

Lemma 2.2 [10] The following inequality for any real value vector $(\phi^0, \phi^1, \dots, \phi^N) \in \mathbb{R}^{N+1}$, $N \in \mathbb{N}$ holds:

$$\sum_{p=0}^N \left[\sum_{k=0}^p \xi_k^{\varsigma-1} \phi^{p-k} \right] \phi^p \geq 0, \quad \varsigma \in (1, 2]. \tag{2.10}$$

Lemma 2.3 [18] Assume that $u \in J_S^\circ(\Gamma)$ be the closure of $C_0^\infty(\mathbb{R}^2)$ with the norm

$$\|u\|_{J_S^\circ(\Gamma)} = \sqrt{\|u\|_{L^2(\Gamma)}^2 + |u|_{J_S^\circ(\Gamma)}^2}, \quad o \in (1, 2),$$

where $|u|_{J_S^\circ(\Gamma)}$ is the semi-norm and defined by

$$|u|_{J_S^\circ(\Gamma)} = \sqrt{|({}^R_a D_x^o u, {}^R_x D_b^o u)_{L^2(\Gamma)}|^2 + |({}^R_c D_y^o u, {}^R_y D_d^o u)_{L^2(\Gamma)}|^2}.$$

Also, let \bar{u} is the expansion of u by zero outside of Γ . Then, the following relationships are established:

$$\begin{aligned} ({}^R_x D_L^o u, {}^R_x D_R^o u)_{L^2(\Gamma)} &= ({}^R_x D_L^o \bar{u}, {}^R_{L_x} D_R^o \bar{u})_{L^2(\mathbb{R}^2)} = \cos(\pi o) \|{}^R_x D_L^o \bar{u}\|_{L^2(\mathbb{R}^2)}, \\ ({}^R_y D_L^o u, {}^R_y D_R^o u)_{L^2(\Gamma)} &= ({}^R_y D_L^o \bar{u}, {}^R_{y} D_R^o \bar{u})_{L^2(\mathbb{R}^2)} = \cos(\pi o) \|{}^R_y D_L^o \bar{u}\|_{L^2(\mathbb{R}^2)}. \end{aligned}$$

Lemma 2.4 [18] Assume that $u, u_1 \in J_L^\circ(\Gamma)$, $o \in (1, 2)$ such that u over the interval $\partial\Gamma$ is equal to zero and $u_1|_{\partial\Gamma} = 0$. Here $J_L^\circ(\Gamma)$ is the closure of $C_0^\infty(\mathbb{R}^2)$ with the norm

$$\|u\|_{J_L^\circ(\Gamma)} = \sqrt{\|u\|_{L^2(\Gamma)}^2 + |u|_{J_L^\circ(\Gamma)}^2}, \quad o \in (1, 2),$$

in which $|u|_{J_L^\circ(\Gamma)}$ denotes the semi-norm and defined by

$$|u|_{J_L^\circ(\Gamma)} = \sqrt{\|{}^R_a D_x^o u\|_{L^2(\Gamma)}^2 + \|{}^R_c D_y^o u\|_{L^2(\Gamma)}^2}.$$

Then,

$$\begin{aligned} ({}^R_a D_x^o u, u_1) &= ({}^R_a D_x^{\frac{o}{2}} u, {}^R_x D_b^{\frac{o}{2}} u_1), \quad ({}^R_c D_y^o u, u_1) = ({}^R_c D_y^{\frac{o}{2}} u, {}^R_y D_d^{\frac{o}{2}} u_1), \\ ({}^R_x D_b^o u, u_1) &= ({}^R_x D_b^{\frac{o}{2}} u, {}^R_a D_x^{\frac{o}{2}} u_1), \quad ({}^R_y D_d^o u, u_1) = ({}^R_y D_d^{\frac{o}{2}} u, {}^R_c D_y^{\frac{o}{2}} u_1). \end{aligned}$$

Definition 2.5 [18] Let $o \in (1, 2)$. Then, we introduce the semi-norm

$$|u|_{\mathbb{H}^o(\mathbb{R}^2)} = \| |s|^o \hat{u}(s) \|_{L^2(\mathbb{R}_s^2)},$$

where $\hat{u}(s)$ is the Fourier transform of u and the following norm

$$\|u\|_{\mathbb{H}^0(\mathbb{R}^2)} = \sqrt{\|u\|_{L^2(\mathbb{R}^2)}^2 + |u|_{\mathbb{H}^0(\mathbb{R}^2)}^2},$$

in which $\mathbb{H}^0(\mathbb{R}^2)$ is the closure of $C_0^\infty(\mathbb{R}^2)$.

Lemma 2.6 [45] Assume that ψ_k for $k = 1, 2, \dots$ are the non-negative sequences such that the sequence z_k satisfies

$$\begin{aligned} z_0 &\leq a_0, \\ z_n &\leq a_0 + \sum_{l=0}^{n-1} c_l + \sum_{l=0}^{n-1} \psi_l z_l, \quad n = 1, 2, \dots \end{aligned}$$

Then, the sequence z_k satisfies

$$\begin{aligned} z_1 &\leq a_0(1 + \psi_0) + c_0, \\ z_n &\leq a_0 \prod_{l=0}^{n-1} (1 + \psi_l) + \sum_{l=0}^{n-2} c_l \prod_{k=l+1}^{n-1} (1 + \psi_k) + c_{n-1}, \quad n = 2, 3, \dots \end{aligned}$$

Furthermore, if $a_0 \geq 0$ and $c_0 \geq 0$, we have the following inequality:

$$z_n \leq \left[a_0 + \sum_{l=0}^{n-1} c_l \right] e^{\sum_{l=0}^{n-1} \psi_l}, \quad n = 1, 2, \dots$$

To solve the equation (1.1) by using of the midpoint quadrature formula combined with the linear B-spline interpolation and Galerkin finite element numerical methods, we can be rewritten its equation as below:

$$\int_0^1 b(\beta)^C D_t^\beta w(x, y, t) d\beta = I_t^{\mu-1, \omega} \left[\mathbf{A}_x \frac{\partial^\eta w(x, y, t)}{\partial |x|^\eta} + \mathbf{A}_y \frac{\partial^v w(x, y, t)}{\partial |y|^v} \right] + g(x, y, t). \tag{2.11}$$

By setting the value $t_{n-\frac{1}{2}}$ into Eq. (2.11) and applying the Lemma 2.1, Eq. (2.7), we obtain the following relation:

$$\begin{aligned} \sum_{j=0}^n \mathbf{b}_{j, n-\frac{1}{2}} \frac{\partial w(x, y, t_j)}{\partial t} + \mathcal{O}(h^2 + (\Delta t)^{2+\frac{h}{2}}) &= (\Delta t)^{\mu-1} \sum_{l=0}^n \xi_l^{\mu-1} \left[\mathbf{A}_x \frac{\partial^\eta w(x, y, t_{n-l-\frac{1}{2}})}{\partial |x|^\eta} + \mathbf{A}_y \frac{\partial^v w(x, y, t_{n-l-\frac{1}{2}})}{\partial |y|^v} \right] \\ &+ g(x, y, t_{n-\frac{1}{2}}) + \mathcal{O}((\Delta t)^2), \quad n = 1, 2, \dots \end{aligned} \tag{2.12}$$

Let $w(x, y, t_j) = w^j$ and $g(x, y, t_j) = g^j$, then we can be written Eq. (2.12) as

$$\begin{aligned} \sum_{j=0}^n \mathbf{b}_{j, n-\frac{1}{2}} \frac{\partial w^j}{\partial t} + \mathcal{O}(h^2 + (\Delta t)^{2+\frac{h}{2}}) &= (\Delta t)^{\mu-1} \sum_{l=0}^n \xi_l^{\mu-1} \left[\mathbf{A}_x \frac{\partial^\eta w^{n-l-\frac{1}{2}}}{\partial |x|^\eta} + \mathbf{A}_y \frac{\partial^v w^{n-l-\frac{1}{2}}}{\partial |y|^v} \right] \\ &+ g^{n-\frac{1}{2}} + \mathcal{O}((\Delta t)^2), \quad n = 1, 2, \dots \end{aligned} \tag{2.13}$$

We can be transformed the above equation into the following form:

$$\sum_{j=0}^n \mathbf{b}_{j, n-\frac{1}{2}} \frac{\partial w^j}{\partial t} = (\Delta t)^{\mu-1} \sum_{l=0}^n \xi_l^{\mu-1} \left[\mathbf{A}_x \frac{\partial^\eta w^{n-l-\frac{1}{2}}}{\partial |x|^\eta} + \mathbf{A}_y \frac{\partial^v w^{n-l-\frac{1}{2}}}{\partial |y|^v} \right] + g^{n-\frac{1}{2}} + \mathcal{O}(h^2 + (\Delta t)^2 + (\Delta t)^{2+\frac{h}{2}}), \quad n = 1, 2, \dots \tag{2.14}$$

By taking inner product of (2.14) with $\varphi \in \mathbb{H}_0^\eta \cap \mathbb{H}_0^v$ and omitting the expression $\mathcal{O}(h^2 + (\Delta t)^2 + (\Delta t)^{2+\frac{h}{2}})$, we have

$$\sum_{j=0}^n \mathbf{b}_{j, n-\frac{1}{2}} \left(\frac{\partial w^j}{\partial t}, \varphi \right) = (\Delta t)^{\mu-1} \sum_{l=0}^n \xi_l^{\mu-1} \left[\left(\mathbf{A}_x \frac{\partial^\eta w^{n-l-\frac{1}{2}}}{\partial |x|^\eta}, \varphi \right) + \left(\mathbf{A}_y \frac{\partial^v w^{n-l-\frac{1}{2}}}{\partial |y|^v}, \varphi \right) \right] + \left(g^{n-\frac{1}{2}}, \varphi \right). \tag{2.15}$$

With help of the definition of the Riesz fractional operator and the Lemma 2.4, we get

$$\begin{aligned} \sum_{j=0}^n \mathbf{b}_{j, n-\frac{1}{2}} \left(\frac{\partial w^j}{\partial t}, \varphi \right) &+ (\Delta t)^{\mu-1} \sum_{l=0}^n \xi_l^{\mu-1} \left[A_\eta \mathbf{A}_x \left({}^{RL}D_x^{\frac{\eta}{2}} w^{n-l-\frac{1}{2}}, {}^{RL}D_b^{\frac{\eta}{2}} \varphi \right) + \left({}^{RL}D_b^{\frac{\eta}{2}} w^{n-l-\frac{1}{2}}, {}^{RL}D_x^{\frac{\eta}{2}} \varphi \right) \right] \\ &+ A_v \mathbf{A}_y \left({}^{RL}D_y^{\frac{v}{2}} w^{n-l-\frac{1}{2}}, {}^{RL}D_d^{\frac{v}{2}} \varphi \right) + \left({}^{RL}D_d^{\frac{v}{2}} w^{n-l-\frac{1}{2}}, {}^{RL}D_y^{\frac{v}{2}} \varphi \right) \\ &= \left(g^{n-\frac{1}{2}}, \varphi \right) \end{aligned} \tag{2.16}$$

where $A_\eta = \frac{1}{2\cos(\frac{\pi\eta}{2})}$ and $A_\nu = \frac{1}{2\cos(\frac{\pi\nu}{2})}$. Thus, we obtain the following variational weak formula for any $\varphi \in \mathbb{H}_0^\eta \cap \mathbb{H}_0^\nu$:

$$\sum_{j=0}^n \mathbf{b}_{j,n-\frac{1}{2}} \left(\frac{\partial w^j}{\partial t}, \varphi \right) + (\Delta t)^{\mu-1} \sum_{l=0}^n \xi_l^{\mu-1} \mathfrak{B}(w^{n-l-\frac{1}{2}}, \varphi) = (g^{n-\frac{1}{2}}, \varphi), \tag{2.17}$$

where

$$\mathfrak{B}(w, \varphi) = \left[A_\eta \mathbf{A}_x \left(({}^R D_x^{\frac{\eta}{2}} w, {}^R D_b^{\frac{\eta}{2}} \varphi) + ({}^R D_b^{\frac{\eta}{2}} w, {}^R D_x^{\frac{\eta}{2}} \varphi) \right) + A_\nu \mathbf{A}_y \left(({}^R D_y^{\frac{\nu}{2}} w, {}^R D_d^{\frac{\nu}{2}} \varphi) + ({}^R D_d^{\frac{\nu}{2}} w, {}^R D_y^{\frac{\nu}{2}} \varphi) \right) \right],$$

and we find $w^n \in \mathbb{H}_0^\eta \cap \mathbb{H}_0^\nu$ such that it satisfy in the equation (2.17).

Theorem 2.7 Suppose that $w^n \in \mathbb{H}_0^\eta \cap \mathbb{H}_0^\nu$. Then the variational weak formula given in (2.17) is unconditionally stable.

Proof. Putting $\varphi = w^{n-\frac{1}{2}}$ in the equation (2.17), we obtain

$$\sum_{j=0}^n \mathbf{b}_{j,n-\frac{1}{2}} \left(\frac{\partial w^j}{\partial t}, w^{n-\frac{1}{2}} \right) + (\Delta t)^{\mu-1} \sum_{l=0}^n \xi_l^{\mu-1} \mathfrak{B}(w^{n-l-\frac{1}{2}}, w^{n-\frac{1}{2}}) = (g^{n-\frac{1}{2}}, w^{n-\frac{1}{2}}). \tag{2.18}$$

With a simple calculation, the left-hand side relations of Eq. (2.18) can rewritten as below:

$$\begin{aligned} \sum_{j=0}^n \mathbf{b}_{j,n-\frac{1}{2}} \left(\frac{\partial w^j}{\partial t}, w^{n-\frac{1}{2}} \right) &= \sum_{j=0}^n \mathbf{b}_{j,n-\frac{1}{2}} \int_\Gamma \left(\frac{w^j - w^{j-1}}{\Delta t} \right) \left(\frac{w^n + w^{n-1}}{2} \right) d\Gamma \\ &= \frac{\mathbf{b}_{n,n-\frac{1}{2}}}{2\Delta t} \int_\Gamma (w^n - w^{n-1})(w^n + w^{n-1}) d\Gamma \\ &= \frac{\mathbf{b}_{n,n-\frac{1}{2}}}{2\Delta t} \left(\|w^n\|_{L^2(\Gamma)}^2 - \|w^{n-1}\|_{L^2(\Gamma)}^2 \right), \end{aligned} \tag{2.19}$$

and

$$\begin{aligned} \sum_{l=0}^n \xi_l^{\mu-1} \mathfrak{B}(w^{n-l-\frac{1}{2}}, w^{n-\frac{1}{2}}) &= A_\eta \mathbf{A}_x \sum_{l=0}^n \xi_l^{\mu-1} \left(({}^R D_x^{\frac{\eta}{2}} w^{n-l-\frac{1}{2}}, {}^R D_b^{\frac{\eta}{2}} w^{n-\frac{1}{2}}) + ({}^R D_b^{\frac{\eta}{2}} w^{n-l-\frac{1}{2}}, {}^R D_x^{\frac{\eta}{2}} w^{n-\frac{1}{2}}) \right) \\ &\quad + A_\nu \mathbf{A}_y \sum_{l=0}^n \xi_l^{\mu-1} \left(({}^R D_y^{\frac{\nu}{2}} w^{n-l-\frac{1}{2}}, {}^R D_d^{\frac{\nu}{2}} w^{n-\frac{1}{2}}) + ({}^R D_d^{\frac{\nu}{2}} w^{n-l-\frac{1}{2}}, {}^R D_y^{\frac{\nu}{2}} w^{n-\frac{1}{2}}) \right). \end{aligned} \tag{2.20}$$

Thus, we check one of the expressions displayed in Eq. (2.19), for example

$$\sum_{l=0}^n \xi_l^{\mu-1} ({}^R D_x^{\frac{\eta}{2}} w^{n-l-\frac{1}{2}}, {}^R D_b^{\frac{\eta}{2}} w^{n-\frac{1}{2}}),$$

Therefore,

$$\begin{aligned} \sum_{n=0}^N \sum_{l=0}^n \xi_l^{\mu-1} ({}^R D_x^{\frac{\eta}{2}} w^{n-l-\frac{1}{2}}, {}^R D_b^{\frac{\eta}{2}} w^{n-\frac{1}{2}}) &= \sum_{n=0}^N \sum_{l=0}^n \xi_l^{\mu-1} \int_\Gamma [{}^R D_x^{\frac{\eta}{2}} w^{n-l-\frac{1}{2}}] [{}^R D_b^{\frac{\eta}{2}} w^{n-\frac{1}{2}}] d\Gamma \\ &= \int_\Gamma \left(\sum_{n=0}^N \left[\sum_{l=0}^n \xi_l^{\mu-1} ({}^R D_x^{\frac{\eta}{2}} w^{n-l-\frac{1}{2}}) \right] ({}^R D_b^{\frac{\eta}{2}} w^{n-\frac{1}{2}}) \right) d\Gamma. \end{aligned} \tag{2.21}$$

From the Lemma 2.2, we conclude that

$$\sum_{n=0}^N \sum_{l=0}^n \xi_l^{\mu-1} ({}^R D_x^{\frac{\eta}{2}} w^{n-l-\frac{1}{2}}, {}^R D_b^{\frac{\eta}{2}} w^{n-\frac{1}{2}}) \geq 0,$$

so

$$\sum_{n=0}^N \sum_{l=0}^n \xi_l^{\mu-1} \mathfrak{B}(w^{n-l-\frac{1}{2}}, w^{n-\frac{1}{2}}) \geq 0. \tag{2.22}$$

By summing Eq. (2.18), from $n = 0$ to N , we can obtain

$$\sum_{n=0}^N \left(\frac{\mathbf{b}_{n,n-\frac{1}{2}}}{2\Delta t} \left(\|w^n\|_{L^2(\Gamma)}^2 - \|w^{n-1}\|_{L^2(\Gamma)}^2 \right) \right) + (\Delta t)^{\mu-1} \sum_{n=0}^N \sum_{l=0}^n \xi_l^{\mu-1} \mathfrak{B}(w^{n-l-\frac{1}{2}}, w^{n-\frac{1}{2}}) = \sum_{n=0}^N (g^{n-\frac{1}{2}}, w^{n-\frac{1}{2}}), \tag{2.23}$$

Applying Eqs. (2.19) and (2.22), we have

$$\begin{aligned} \frac{\mathbf{b}_{N,N-\frac{1}{2}}}{2\Delta t} \left(\|w^N\|_{L^2(\Gamma)}^2 - \|w^0\|_{L^2(\Gamma)}^2 \right) &\leq \frac{\mathbf{b}_{N,N-\frac{1}{2}}}{2\Delta t} \left(\|w^N\|_{L^2(\Gamma)}^2 - \|w^0\|_{L^2(\Gamma)}^2 \right) + (\Delta t)^{\mu-1} \sum_{n=0}^N \sum_{l=0}^n \xi_l^{\mu-1} \mathfrak{B}(w^{n-l-\frac{1}{2}}, w^{n-\frac{1}{2}}) \\ &= \sum_{n=0}^N (g^{n-\frac{1}{2}}, w^{n-\frac{1}{2}}). \end{aligned} \tag{2.24}$$

Now, we change the index of the series given above from N to n , then

$$\|w^n\|_{L^2(\Gamma)}^2 - \|w^0\|_{L^2(\Gamma)}^2 \leq \frac{2\Delta t}{\mathbf{b}_{n,n-\frac{1}{2}}} \sum_{i=0}^n (g^{i-\frac{1}{2}}, w^{n-\frac{1}{2}}). \tag{2.25}$$

By using the Cauchy-Schwarz inequality, the formula (2.25) can be displayed as

$$\begin{aligned} \|w^n\|_{L^2(\Gamma)}^2 - \|w^0\|_{L^2(\Gamma)}^2 &\leq \frac{2\Delta t}{\mathbf{b}_{n,n-\frac{1}{2}}} \sum_{i=0}^n (g^{i-\frac{1}{2}}, w^{n-\frac{1}{2}}) \\ &\leq \frac{\Delta t}{\mathbf{b}_{n,n-\frac{1}{2}}} \left[\sum_{i=0}^n \|g^{i-\frac{1}{2}}\|_{L^2(\Gamma)}^2 + \sum_{i=0}^n \|w^{n-\frac{1}{2}}\|_{L^2(\Gamma)}^2 \right]. \end{aligned} \tag{2.26}$$

By applying the Lemma 2.6, the following inequality is obtained:

$$\begin{aligned} \|w^n\|_{L^2(\Gamma)}^2 &\leq \left[\|w^0\|_{L^2(\Gamma)}^2 + \frac{\Delta t}{\mathbf{b}_{n,n-\frac{1}{2}}} \sum_{i=0}^n \|g^{i-\frac{1}{2}}\|_{L^2(\Gamma)}^2 \right] e^{\frac{\Delta t}{\mathbf{b}_{n,n-\frac{1}{2}}}} \\ &\leq \left[\|w^0\|_{L^2(\Gamma)}^2 + \frac{n\Delta t}{\mathbf{b}_{n,n-\frac{1}{2}}} \max_{1 \leq i \leq n} \|g^{i-\frac{1}{2}}\|_{L^2(\Gamma)}^2 \right] e^{\frac{\Delta t}{\mathbf{b}_{n,n-\frac{1}{2}}}} \\ &\left[\|w^0\|_{L^2(\Gamma)}^2 + \frac{T}{\mathbf{b}_{n,n-\frac{1}{2}}} \max_{1 \leq i \leq n} \|g^{i-\frac{1}{2}}\|_{L^2(\Gamma)}^2 \right] e^{\frac{\Delta t}{\mathbf{b}_{n,n-\frac{1}{2}}}} \\ &\leq \mathbb{K}_1 \|w^0\|_{L^2(\Gamma)}^2 + \mathbb{K}_2 \max_{1 \leq i \leq n} \|g^{i-\frac{1}{2}}\|_{L^2(\Gamma)}^2. \end{aligned} \tag{2.27}$$

So, the proof is completed. □

3 Convergence analysis study for the full-discrete method

Define the domain Γ_ϑ as follows:

$$\Gamma_\vartheta = \{e_\vartheta : e_\vartheta \in \mathbb{T}_\vartheta\},$$

in which \mathbb{T}_ϑ denotes the triangulation domains and ϑ is the maximum diameter for the triangulation domains. Furthermore, suppose that finite element subspace \mathbf{X}_ϑ^k is defined by the following set:

$$\mathbf{X}_\vartheta^l = \{\Xi_\vartheta \in C(\tilde{\Gamma}), \Xi_\vartheta|_{\partial\Gamma} = 0, \Xi_\vartheta|_e = \nabla_l(x, y), \Xi_\vartheta|_{(x,y) \neq e} = 0\},$$

where the ∇_l are the space of linear-piecewise continuous functions. Let P_ϑ^m be a interpolation operator. Then, for any $w \in J^r(\Gamma)$, we can obtain the following approximate:

$$\|w - P_\vartheta^m w\| \leq C\vartheta^{m-r} \|w\|_{J^m(\Gamma)}, \quad r = 0, 1, \dots, m. \tag{3.1}$$

We assume that $\Upsilon_\vartheta : J_0^\eta(\Gamma) \rightarrow \mathbf{X}_\vartheta^k$ be the projection operator which is defined by the following map:

$$\mathfrak{B}(\Upsilon_\vartheta w, \varphi) = \mathfrak{B}(w, \varphi), \quad \varphi \in \mathbf{X}_\vartheta^l. \tag{3.2}$$

Lemma 3.1 [5] For $w \in J^\alpha \cap J_0^\eta$ that $\eta \leq \alpha \leq l + 1$, the following inequality is valid:

$$\|w - \Upsilon_\vartheta w\| C\vartheta^{\alpha-\eta} \|w\|_{J^\alpha(\Gamma)}. \tag{3.3}$$

By setting the value Ξ_ϑ in the equation (2.17), we get the following variational weak form for the full-discrete method:

$$\sum_{j=0}^n \mathbf{b}_{j,n-\frac{1}{2}} \left(\frac{\partial w^j}{\partial t}, \Xi_\vartheta \right) + (\Delta t)^{\mu-1} \sum_{l=0}^n \xi_l^{\mu-1} \mathfrak{B}(w^{n-l-\frac{1}{2}}, \Xi_\vartheta) = (g^{n-\frac{1}{2}}, \Xi_\vartheta). \tag{3.4}$$

Now, we find $W_\vartheta^n \in J^\eta \cap J_0^\nu$ that

$$\sum_{j=0}^n \mathbf{b}_{j,n-\frac{1}{2}} \left(\frac{\partial W_\vartheta^j}{\partial t}, \Xi_\vartheta \right) + (\Delta t)^{\mu-1} \sum_{l=0}^n \xi_l^{\mu-1} \mathfrak{B}(W_\vartheta^{n-l-\frac{1}{2}}, \Xi_\vartheta) = (g^{n-\frac{1}{2}}, \Xi_\vartheta), \tag{3.5}$$

for any $\Xi_\vartheta \in J^\eta \cap J_0^\nu$.

Theorem 3.2 Suppose that w^n is the solutions of the equation (1.1) and W_ϑ^n is the solutions of the equation (3.5). Then, the full-discrete numerical method based on the finite element estimation for Eq. (3.5) is convergent with order $h^2 + (\Delta t)^2 + \vartheta^2$.

Proof For any $\Xi_\vartheta \in J^\eta \cap J_0^\nu$, we have

$$\sum_{j=0}^n \mathbf{b}_{j,n-\frac{1}{2}} \left(\frac{\partial w^j}{\partial t}, \Xi_\vartheta \right) + (\Delta t)^{\mu-1} \sum_{l=0}^n \xi_l^{\mu-1} \mathfrak{B}(w^{n-l-\frac{1}{2}}, \Xi_\vartheta) = (g^{n-\frac{1}{2}}, \Xi_\vartheta) + (R_{\Delta t}, \Xi_\vartheta). \tag{3.6}$$

By subtracting the equation (3.5) from the equation (3.6), for any $\Xi_\vartheta \in J^\eta \cap J_0^\nu$, we obtain

$$\sum_{j=0}^n \mathbf{b}_{j,n-\frac{1}{2}} \left(\frac{\partial(w^j - W^j)}{\partial t}, \Xi_\vartheta \right) + (\Delta t)^{\mu-1} \sum_{l=0}^n \xi_l^{\mu-1} \mathfrak{B}(w^{n-l-\frac{1}{2}} - W^{n-l-\frac{1}{2}}, \Xi_\vartheta) = (R_{\Delta t}, \Xi_\vartheta). \tag{3.7}$$

We consider the following symbols:

$$\Psi_\vartheta^n = w - \Upsilon_\vartheta w^n, \Phi_\vartheta^n = \Upsilon_\vartheta w^n - W_\vartheta^n. \tag{3.8}$$

So the equation (3.7) can be rewritten as follows:

$$\sum_{j=0}^n \mathbf{b}_{j,n-\frac{1}{2}} \left(\frac{\partial \Psi_\vartheta^j}{\partial t}, \Xi_\vartheta \right) + (\Delta t)^{\mu-1} \sum_{l=0}^n \xi_l^{\mu-1} \mathfrak{B}(\Psi_\vartheta^{n-l-\frac{1}{2}}, \Xi_\vartheta) = (R_{\Delta t}, \Xi_\vartheta) - \sum_{j=0}^n \mathbf{b}_{j,n-\frac{1}{2}} \left(\frac{\partial \Phi_\vartheta^j}{\partial t}, \Xi_\vartheta \right). \tag{3.9}$$

Put $\Xi_\vartheta = \Psi_\vartheta^{n-\frac{1}{2}}$ into the equation (3.9), thus

$$\sum_{j=0}^n \mathbf{b}_{j,n-\frac{1}{2}} \left(\frac{\partial \Psi_\vartheta^j}{\partial t}, \Psi_\vartheta^{n-\frac{1}{2}} \right) + (\Delta t)^{\mu-1} \sum_{l=0}^n \xi_l^{\mu-1} \mathfrak{B}(\Psi_\vartheta^{n-l-\frac{1}{2}}, \Psi_\vartheta^{n-\frac{1}{2}}) = (R_{\Delta t}, \Psi_\vartheta^{n-\frac{1}{2}}) - \sum_{j=0}^n \mathbf{b}_{j,n-\frac{1}{2}} \left(\frac{\partial \Phi_\vartheta^j}{\partial t}, \Psi_\vartheta^{n-\frac{1}{2}} \right). \tag{3.10}$$

With a simple calculation, the left-hand side relations of Eq. (3.10) can be rewritten as below:

$$\begin{aligned} \sum_{j=0}^n \mathbf{b}_{j,n-\frac{1}{2}} \left(\frac{\partial \Psi_\vartheta^j}{\partial t}, \Psi_\vartheta^{n-\frac{1}{2}} \right) &= \sum_{j=0}^n \mathbf{b}_{j,n-\frac{1}{2}} \int_\Gamma \left(\frac{\Psi_\vartheta^j - \Psi_\vartheta^{j-1}}{\Delta t} \right) \left(\frac{\Psi_\vartheta^n + \Psi_\vartheta^{n-1}}{2} \right) d\Gamma \\ &= \frac{\mathbf{b}_{n,n-\frac{1}{2}}}{2\Delta t} \int_\Gamma (\Psi_\vartheta^n - \Psi_\vartheta^{n-1})(\Psi_\vartheta^n + \Psi_\vartheta^{n-1}) d\Gamma \\ &= \frac{\mathbf{b}_{n,n-\frac{1}{2}}}{2\Delta t} \left(\|\Psi_\vartheta^n\|_{L^2(\Gamma)}^2 - \|\Psi_\vartheta^{n-1}\|_{L^2(\Gamma)}^2 \right), \end{aligned} \tag{3.11}$$

and

$$\begin{aligned} \sum_{l=0}^n \xi_l^{\mu-1} \mathfrak{B}(\Psi_\vartheta^{n-l-\frac{1}{2}}, \Psi_\vartheta^{n-\frac{1}{2}}) &= A_\eta \mathbf{A}_x \sum_{l=0}^n \xi_l^{\mu-1} \left(({}^{RL}D_x^{\frac{\eta}{2}} \Psi_\vartheta^{n-l-\frac{1}{2}}, {}^{RL}D_b^{\frac{\eta}{2}} \Psi_\vartheta^{n-\frac{1}{2}}) + ({}^{RL}D_b^{\frac{\eta}{2}} \Psi_\vartheta^{n-l-\frac{1}{2}}, {}^{RL}D_x^{\frac{\eta}{2}} \Psi_\vartheta^{n-\frac{1}{2}}) \right) \\ &\quad + A_\nu \mathbf{A}_y \sum_{l=0}^n \xi_l^{\mu-1} \left(({}^{RL}D_y^{\frac{\nu}{2}} \Psi_\vartheta^{n-l-\frac{1}{2}}, {}^{RL}D_d^{\frac{\nu}{2}} \Psi_\vartheta^{n-\frac{1}{2}}) + ({}^{RL}D_d^{\frac{\nu}{2}} \Psi_\vartheta^{n-l-\frac{1}{2}}, {}^{RL}D_y^{\frac{\nu}{2}} \Psi_\vartheta^{n-\frac{1}{2}}) \right). \end{aligned} \tag{3.12}$$

Thus, we check one of the expressions displayed in Eq. (3.12), for example

$$\sum_{l=0}^n \xi_l^{\mu-1} ({}^{RL}D_x^{\frac{\eta}{2}} \Psi_\vartheta^{n-l-\frac{1}{2}}, {}^{RL}D_b^{\frac{\eta}{2}} \Psi_\vartheta^{n-\frac{1}{2}}),$$

Therefore

$$\begin{aligned} \sum_{n=0}^N \sum_{l=0}^n \xi_l^{\mu-1} ({}^{RL}D_x^{\frac{\eta}{2}} \Psi_\vartheta^{n-l-\frac{1}{2}}, {}^{RL}D_b^{\frac{\eta}{2}} \Psi_\vartheta^{n-\frac{1}{2}}) &= \sum_{n=0}^N \sum_{l=0}^n \xi_l^{\mu-1} \int_{\Gamma} [{}^{RL}D_x^{\frac{\eta}{2}} \Psi_\vartheta^{n-l-\frac{1}{2}}] [{}^{RL}D_b^{\frac{\eta}{2}} \Psi_\vartheta^{n-\frac{1}{2}}] d\Gamma \\ &= \int_{\Gamma} \left(\sum_{n=0}^N \left[\sum_{l=0}^n \xi_l^{\mu-1} {}^{RL}D_x^{\frac{\eta}{2}} \Psi_\vartheta^{n-l-\frac{1}{2}} \right] {}^{RL}D_b^{\frac{\eta}{2}} \Psi_\vartheta^{n-\frac{1}{2}} \right) d\Gamma. \end{aligned} \tag{3.13}$$

From the Lemma 2.2, we conclude that

$$\sum_{n=0}^N \sum_{l=0}^n \xi_l^{\mu-1} ({}^{RL}D_x^{\frac{\eta}{2}} \Psi_\vartheta^{n-l-\frac{1}{2}}, {}^{RL}D_b^{\frac{\eta}{2}} \Psi_\vartheta^{n-\frac{1}{2}}) \geq 0,$$

so

$$\sum_{n=0}^N \sum_{l=0}^n \xi_l^{\mu-1} \mathfrak{B}(\Psi_\vartheta^{n-l-\frac{1}{2}}, \Psi_\vartheta^{n-\frac{1}{2}}) \geq 0. \tag{3.14}$$

Due to the above equations, we have the following formula:

$$\begin{aligned} \frac{1}{2\Delta t} \sum_{n=1}^N \mathbf{b}_{n,n-\frac{1}{2}} \left(\|\Psi_\vartheta^n\|_{L^2(\Gamma)}^2 - \|\Psi_\vartheta^{n-1}\|_{L^2(\Gamma)}^2 \right) &\leq \sum_{n=1}^N \left(\mathbf{R}_{\Delta t}, \Psi_\vartheta^{n-\frac{1}{2}} \right) - \sum_{n=1}^N \sum_{j=0}^n \mathbf{b}_{j,n-\frac{1}{2}} \left(\frac{\partial \Phi_\vartheta^j}{\partial t}, \Psi_\vartheta^{n-\frac{1}{2}} \right) \\ &\leq \sum_{n=1}^N \|\mathbf{R}_{\Delta t}\|_{L^2(\Gamma)}^2 + \sum_{n=1}^N \sum_{j=0}^n \mathbf{b}_{j,n-\frac{1}{2}} \left\| \frac{\partial \Phi_\vartheta^j}{\partial t} \right\|_{L^2(\Gamma)}^2 + \frac{1}{2} \sum_{n=1}^N \|\Psi_\vartheta^{n-\frac{1}{2}}\|_{L^2(\Gamma)}^2 \\ &\leq c_1 \left(h^2 + (\Delta t)^{2+\frac{h}{2}} \right)^2 n + c_2 n \left((\Delta t)^2 + \vartheta^2 \right)^2 + \frac{1}{2} \sum_{n=1}^N \|\Psi_\vartheta^{n-\frac{1}{2}}\|_{L^2(\Gamma)}^2. \end{aligned} \tag{3.15}$$

Then,

$$\mathbf{b}_{N,N-\frac{1}{2}} \left(\|\Psi_\vartheta^N\|_{L^2(\Gamma)}^2 - \|\Psi_\vartheta^0\|_{L^2(\Gamma)}^2 \right) \leq c_1 \left(h^2 + (\Delta t)^{2+\frac{h}{2}} \right)^2 T + c_2 T \left((\Delta t)^2 + \vartheta^2 \right)^2 + \Delta t \sum_{n=1}^N \|\Psi_\vartheta^{n-\frac{1}{2}}\|_{L^2(\Gamma)}^2. \tag{3.16}$$

Because $\Psi_\vartheta^0 = 0$ and by moving the index N to n , the equation (3.16) can be changed to

$$\sqrt{\mathbf{b}_{n,n-\frac{1}{2}}} \|\Psi_\vartheta^n\|_{L^2(\Gamma)} \leq \sqrt{cT} \left(h^2 + (\Delta t)^2 + \vartheta^2 \right) + 2\Delta t \sum_{i=1}^n \|\Psi_\vartheta^i\|_{L^2(\Gamma)}. \tag{3.17}$$

Using Lemma 2.6, we have

$$\|\Psi_\vartheta^n\|_{L^2(\Gamma)} \leq \frac{\sqrt{cT}}{\sqrt{\mathbf{b}_{n,n-\frac{1}{2}}}} \left(h^2 + (\Delta t)^2 + \vartheta^2 \right) e^{\frac{2\Delta t}{\sqrt{\mathbf{b}_{n,n-\frac{1}{2}}}}} \leq C \left(h^2 + (\Delta t)^2 + \vartheta^2 \right). \tag{3.18}$$

Thus, it completes the proof. □

4 Numerical examples

This part studies and discusses the numerical examples using the proposed method to verify and show the efficiency and performance of the proposed method. Furthermore, in this part, the computational order is studied that the computational order (CO) formula is calculated with the following formula:

$$CO = \frac{\log \left(\frac{E_1}{E_2} \right)}{\log \left(\frac{\vartheta_1}{\vartheta_2} \right)},$$

where E_1 and E_2 are the computed error applying the proposed method in the space-sizes ϑ_1 and ϑ_2 , respectively.

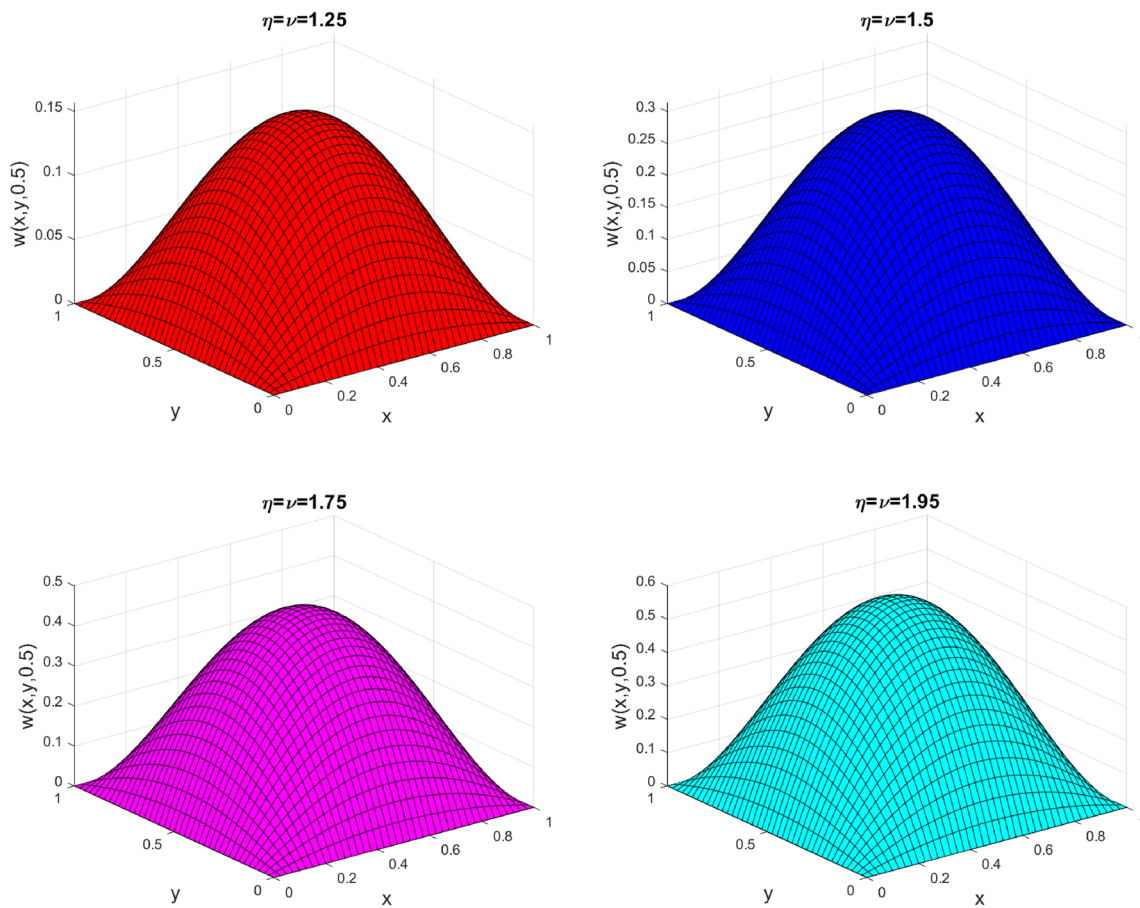


Fig. 2 Graph of the numerical solution for Example 4.1 with different kinds of η and ν with $\omega = 0.5$ and $\mu = 1.5$

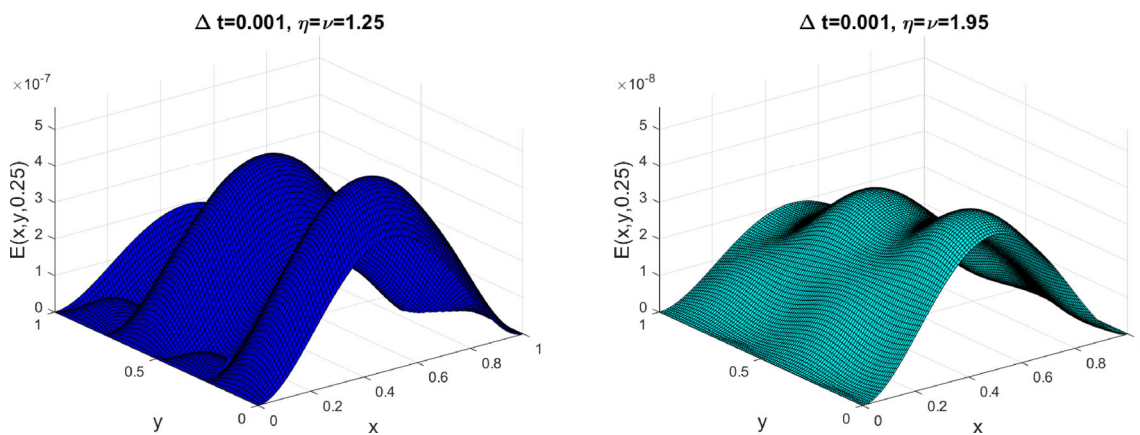


Fig. 3 Graph of the numerical solution for Example 4.1 with different kinds of η and ν with $\omega = 0.5$ and $\mu = 1.5$

Example 4.1 Let us consider the following distributed-order time-fractional diffusion-wave equations with the Riesz space fractional derivatives:

$$\int_0^1 \Gamma(2 - \beta)^C D_t^\beta w(x, y, t) d\beta = \frac{1}{\Gamma(\mu - 1)} \int_0^t (t - \tau)^{\mu-2} e^{-\omega(t-\tau)} \frac{\partial^\eta w(x, y, \tau)}{\partial |x|^\eta} d\tau + \frac{2}{\Gamma(\mu - 1)} \int_0^t (t - \tau)^{\mu-2} e^{-\omega(t-\tau)} \frac{\partial^\nu w(x, y, \tau)}{\partial |y|^\nu} d\tau + g(x, y, t),$$

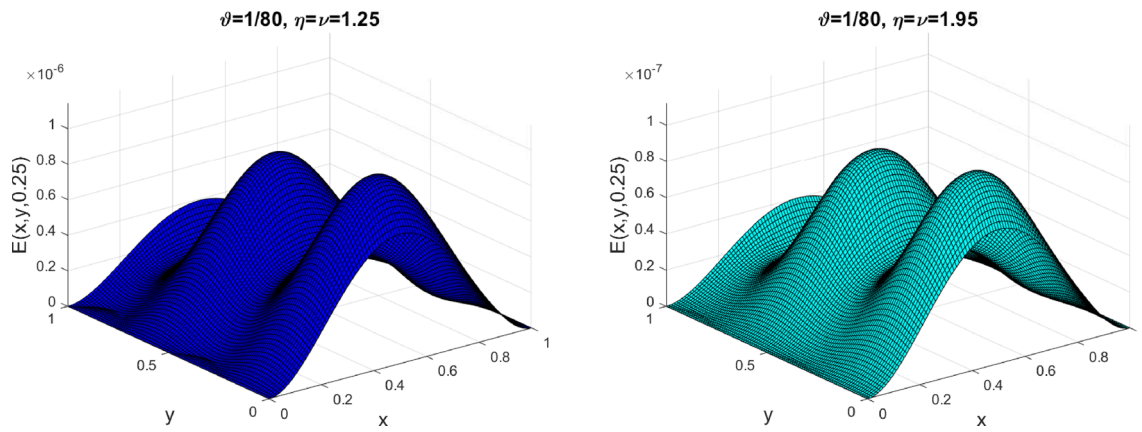


Fig. 4 Graph of the numerical solution for Example 4.1 with different kinds of η and ν with $\omega = 0.5$ and $\mu = 1.5$

Table 1 Comparison of the L_∞ -errors and CO with $\Delta t = 0.001$ for Example 4.1

ϑ	$\eta = \nu = 1.25$		$\eta = \nu = 1.95$	
	L_∞	CO	L_∞	CO
$\frac{1}{4}$	$7.2022e - 02$	-	$8.2009e - 05$	-
$\frac{1}{8}$	$3.0642e - 02$	1.7064	$3.0075e - 05$	1.9888
$\frac{1}{16}$	$7.0018e - 03$	1.8890	$7.0246e - 06$	1.9519
$\frac{1}{32}$	$2.4575e - 03$	1.9480	$2.6031e - 06$	1.9198
$\frac{1}{64}$	$4.8075e - 04$	2.0011	$5.4111e - 07$	1.9919
$\frac{1}{128}$	$1.1405e - 06$	2.0014	$1.1182e - 07$	2.0076

Table 2 Comparison of the L_∞ -errors and CO with $\vartheta = 1/80$ for Example 4.1

Δt	$\eta = \nu = 1.25$		$\eta = \nu = 1.95$		CPU - time
	L_∞	CO	L_∞	CO	
$\frac{1}{20}$	$2.7670e - 05$	-	$2.7424e - 06$	-	0.335
$\frac{1}{40}$	$6.1025e - 06$	1.9429	$6.1013e - 07$	1.9424	0.398
$\frac{1}{80}$	$2.2142e - 06$	1.9987	$2.2014e - 07$	1.9987	0.5100
$\frac{1}{160}$	$5.5912e - 07$	2.0057	$6.5912e - 08$	2.0057	1.988

under the following initial and boundary conditions:

$$w(x, y, 0) = 0, \quad (x, y) \in [0, 1] \times [0, 1],$$

$$w(x, y, t) = 0, \quad (x, y) \in \partial([0, 1] \times [0, 1]), \quad t \in (0, 0.5],$$

in which

$$g(x, y, t) = 10xy(1-x)(1-y) \frac{t-1}{\ln t} - \frac{5t^{\mu+1} e^{-\omega t} {}_1\Psi_1(\omega t)y(1-y)}{\cos(\eta\pi)} \left[\frac{x^\eta + (1-x)^{1-\eta}}{\Gamma(2-\eta)} - \frac{2x^{2-\eta} + 2(1-x)^{2-\eta}}{\Gamma(3-\eta)} \right] - \frac{5t^{\mu+1} e^{-\omega t} {}_1\Psi_1(\omega t)x(1-x)}{\cos(\nu\pi)} \left[\frac{y^\nu + (1-y)^{1-\nu}}{\Gamma(2-\nu)} - \frac{2y^{2-\nu} + 2(1-y)^{2-\nu}}{\Gamma(3-\nu)} \right].$$

Here ${}_p\Psi_q(t)$ is the generalized Wright function and defined by the following relation:

$${}_p\Psi_q(\omega t) = {}_p\Psi_q \left[\begin{matrix} (a_l, \alpha_l)_{l,p} \\ (b_l, \beta_l)_{l,q} \end{matrix} \middle| \omega t \right] = \sum_{k=0}^{\infty} \frac{\prod_{l=1}^p \Gamma(a_l + \alpha_l k)}{\prod_{j=1}^q \Gamma(b_j + \beta_j k)} \frac{(\omega t)^k}{k!},$$

where for this problem, the values $(a_l, \alpha_l)_{l,p}$ and $(b_l, \beta_l)_{l,q}$ are considered by $(2, 1)_{1,1}$ and $(\mu + 1, 1)_{1,1}$, respectively. The exact solution for this Example is $w(x, y, t) = 10 t xy(1-x)(1-y)$. To calculate the approximate solutions for this example we consider

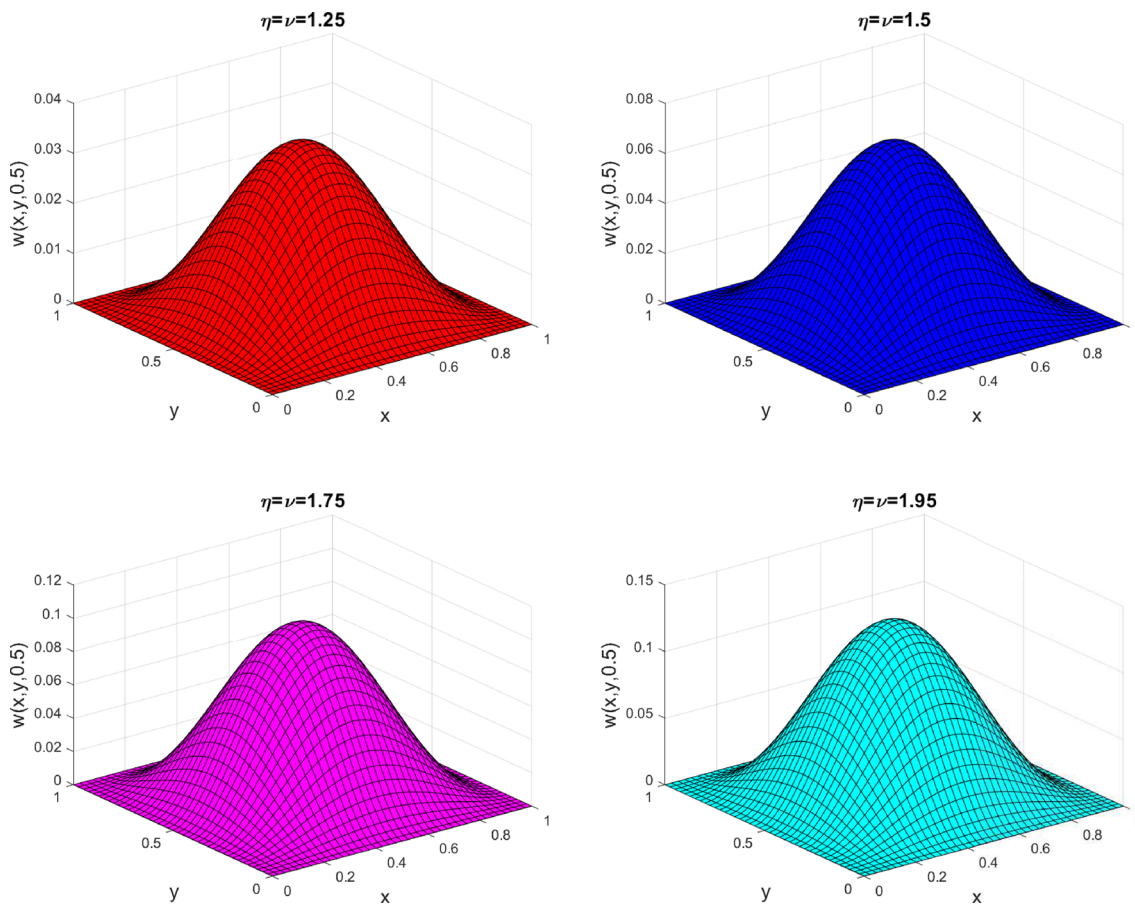


Fig. 5 Graph of the numerical solution for Example 4.2 with different kinds of η and ν with $\omega = 0.5$ and $\mu = 1.5$

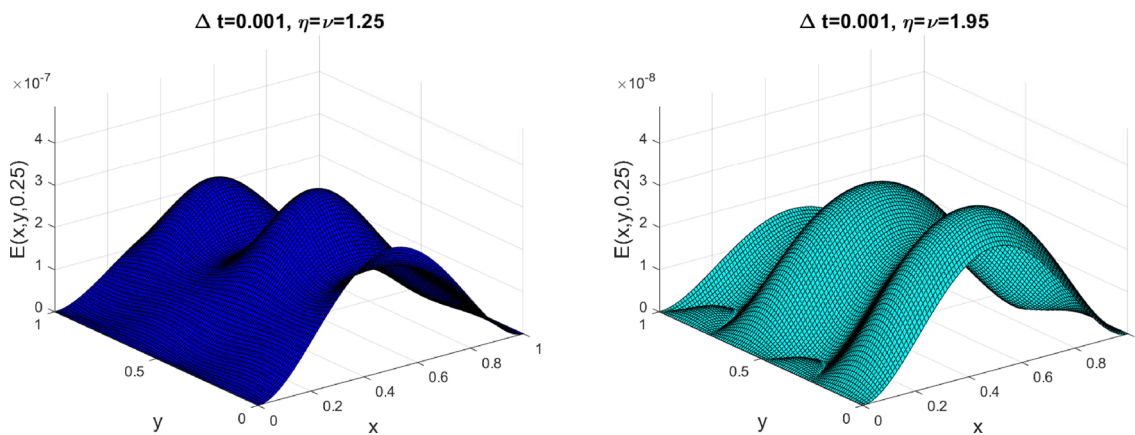


Fig. 6 Graph of the numerical solution for Example 4.2 with different kinds of η and ν with $\omega = 0.5$ and $\mu = 1.5$

$\omega = 0.5$ and $\mu = 1.5$. The initial conditions describe the wave shape and the boundary conditions explicitly enforced on the variational solution and therefore exactly satisfied in the approximate solution. Figure 2 shows the numerical solutions using the proposed method for various choices of η and ν . Figure 3 demonstrates the numerical solutions applying the proposed method for various choices of η and ν when $\vartheta = 1/80$. Figure 4 demonstrates the numerical solutions applying the proposed method for various choices of η and ν when $\Delta t = 0.001$. Table 1 reports the comparison of L_∞ -errors and CO with $\Delta t = 0.001$ for various choices of ϑ . Also, Table 2 displays the comparison of L_∞ -errors and CO with $\vartheta = 1/80$ for various choices of Δt . From the tables shown for this example, we understand that the computational order computed applying the proposed method is second order. From these numerical results which are displayed in Figs. 2, 3 and 4, we seen that the numerical solutions converge to the exact solution.

Example 4.2 We consider following distributed-order time-fractional diffusion-wave equations with the Riesz space fractional derivatives:

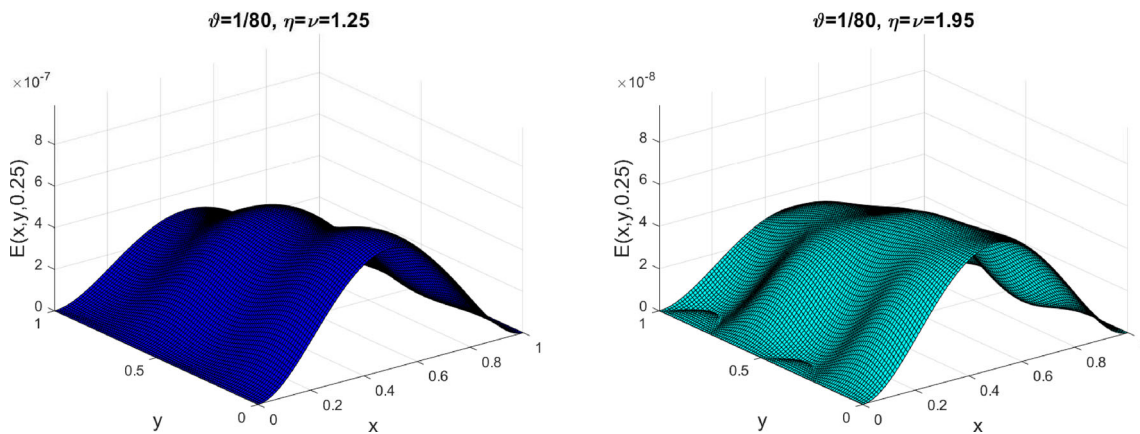


Fig. 7 Graph of the numerical solution for Example 4.2 with different kinds of η and ν with $\omega = 0.5$ and $\mu = 1.5$

Table 3 Comparison of the L_∞ -errors and CO with $\Delta t = 0.001$ for Example 4.2

ϑ	$\eta = \nu = 1.25$		$\eta = \nu = 1.95$	
	L_∞	CO	L_∞	CO
$\frac{1}{4}$	$6.2373e - 02$	–	$8.0373e - 05$	–
$\frac{1}{8}$	$3.0074e - 02$	1.8064	$9.1214e - 06$	1.9998
$\frac{1}{16}$	$7.2240e - 03$	1.9990	$4.0468e - 06$	1.9849
$\frac{1}{32}$	$2.5641e - 03$	1.9890	$2.2117e - 06$	1.9898
$\frac{1}{64}$	$5.1274e - 04$	2.0001	$3.7220e - 07$	1.9999
$\frac{1}{128}$	$2.8423e - 06$	2.0004	$1.3542e - 07$	2.0026

Table 4 Comparison of the L_∞ -errors and CO with $\vartheta = 1/80$ for Example 4.2

Δt	$\eta = \nu = 1.25$		$\eta = \nu = 1.95$		CPU – time
	L_∞	CO	L_∞	CO	
$\frac{1}{20}$	$3.6142e - 05$	–	$8.3104e - 05$	–	0.665
$\frac{1}{40}$	$2.0117e - 05$	1.9659	$2.5676e - 06$	1.9834	0.788
$\frac{1}{80}$	$5.4368e - 06$	1.9997	$4.4777e - 07$	1.9999	0.8420
$\frac{1}{160}$	$5.7726e - 07$	2.0021	$6.8095e - 08$	2.0041	1.999

Table 5 The maximum error calculated by the proposed method for same selections of η and ν for Example 4.2

$\Delta t = \vartheta$	$\eta = \nu = 1.25$	$\eta = \nu = 1.75$	$\eta = \nu = 1.75$
$\frac{1}{10}$	$3.3e - 06$	$2.7e - 06$	$2.3e - 06$
$\frac{1}{20}$	$2.4e - 06$	$2.2e - 06$	$9.1e - 07$
$\frac{1}{40}$	$8.7e - 07$	$6.2e - 07$	$4.3e - 07$
$\frac{1}{160}$	$2.8e - 07$	$2.1e - 07$	$7.7e - 08$

$$\int_0^1 \Gamma\left(\frac{7}{2} - \beta\right)^C D_t^\beta w(x, y, t) d\beta = \frac{4}{\Gamma(\mu - 1)} \int_0^t (t - \tau)^{\mu-2} e^{-\omega(t-\tau)} \frac{\partial^\eta w(x, y, \tau)}{\partial |x|^\eta} d\tau + \frac{3}{\Gamma(\mu - 1)} \int_0^t (t - \tau)^{\mu-2} e^{-\omega(t-\tau)} \frac{\partial^\nu w(x, y, \tau)}{\partial |y|^\nu} d\tau + g(x, y, t),$$

under the following initial and boundary conditions:

$$w(x, y, 0) = 0, \quad (x, y) \in [0, 1] \times [0, 1],$$

$$w(x, y, t) = 0, \quad (x, y) \in \partial([0, 1] \times [0, 1]), \quad t \in (0, 1],$$

in which

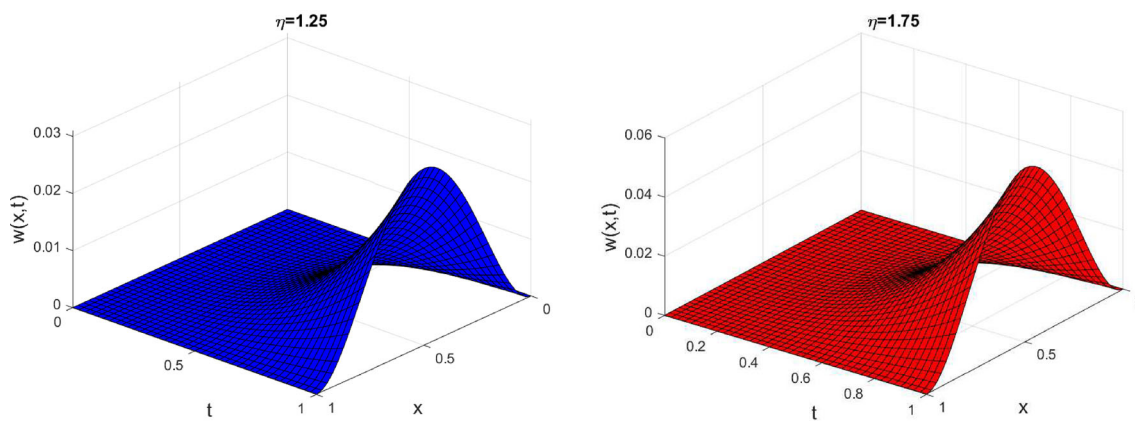


Fig. 8 Graph of the numerical solution for Example 4.3 with different kinds of η with $\omega = 0.1$

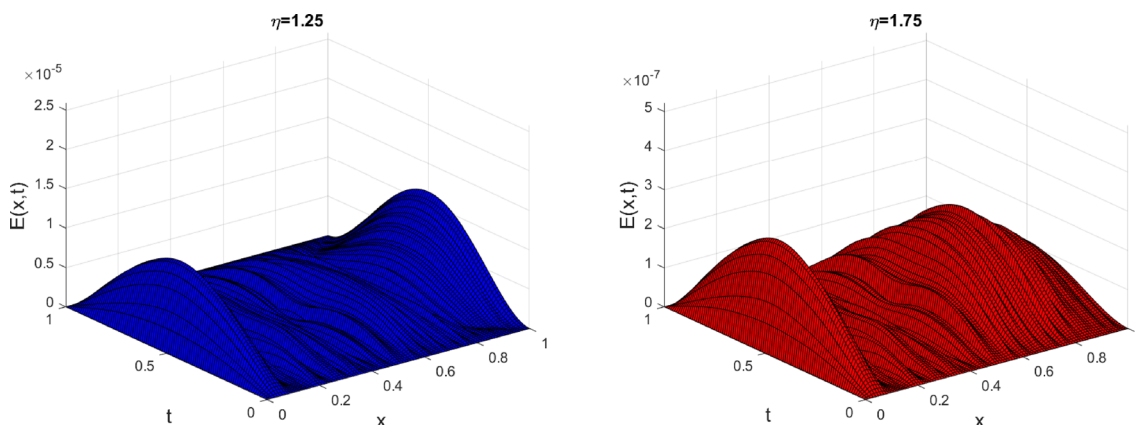


Fig. 9 Graph of the errors for Example 4.3 with different kinds of η with $\omega = 0.1$

$$\begin{aligned}
 g(x, y, t) = & 100(xy(1-x)(1-y))^2 \frac{15\sqrt{\pi}(t^{\frac{5}{2}} - t^{\frac{3}{2}})}{8 \ln t} \\
 & + \frac{400t^{\frac{3}{2}+\mu} e^{-\omega t} (y(1-y))^2}{\cos(\eta\pi)} \left[\frac{x^{2-\eta} + (1-x)^{2-\eta}}{\Gamma(3-\eta)} - \frac{6x^{3-\eta} + 6(1-x)^{3-\eta}}{\Gamma(4-\eta)} \right. \\
 & \left. + \frac{12x^{4-\eta} + 12(1-x)^{4-\eta}}{\Gamma(5-\eta)} \right] {}_1\Psi_1 \left[\begin{matrix} (\frac{7}{2}, 1)_{1,1} \\ (\frac{5}{2} + \mu, 1)_{1,1} \end{matrix} \middle| \omega t \right] \\
 & + \frac{300t^{\frac{3}{2}+\mu} e^{-\omega t} (x(1-x))^2}{\cos(v\pi)} \left[\frac{y^{2-v} + (1-y)^{2-v}}{\Gamma(3-v)} - \frac{6y^{3-v} + 6(1-y)^{3-v}}{\Gamma(4-v)} \right. \\
 & \left. + \frac{12y^{4-v} + 12(1-y)^{4-v}}{\Gamma(5-v)} \right] {}_1\Psi_1 \left[\begin{matrix} (\frac{7}{2}, 1)_{1,1} \\ (\frac{5}{2} + \mu, 1)_{1,1} \end{matrix} \middle| \omega t \right].
 \end{aligned}$$

The exact solution for this Example is $w(x, y, t) = 100 t^{\frac{5}{2}}(xy(1-x)(1-y))^2$. To compute the approximate solutions using the proposed method, we take $\omega = 0.5$ and $\mu = 1.5$. Figure 5 shows the numerical solutions using the proposed method for various choices of η and ν . Figure 6 demonstrates the numerical solutions applying the proposed method for various choices of η and ν when $\vartheta = 1/80$. Figure 7 demonstrates the numerical solutions applying the proposed method for various choices of η and ν when $\Delta t = 0.001$. The comparison of L_∞ -errors and corresponding CO with $\Delta t = 0.001$ for various choices of ϑ is shown in Table 3. Also, Table 4 shows L_∞ -errors and corresponding CO with $\vartheta = 1/80$ for various choices of Δt . The maximum error computed applying the proposed method for this example with the same choices of parameters Δt and ϑ is displayed in Table 5. From the tables shown for this example, we see that the computational order computed applying the proposed method is second order.

Table 6 Comparison of the L_∞ -errors and CO with $\Delta t = 0.001$ for Example 4.3

ϑ	Present method			
	$\eta = \nu = 1.25$		$\eta = \nu = 1.95$	
	L_∞	CO	L_∞	CO
$\frac{1}{4}$	2.5796e-05	–	1.6123e-07	–
$\frac{1}{8}$	3.2245e-06	1.9859	8.0613e-08	1.9899
$\frac{1}{16}$	1.6123e-06	2.0011	4.0306e-08	2.0018
$\frac{1}{32}$	8.0613e-07	2.0020	2.0153e-08	2.0023
ϑ	Proposed method in [16]			
	$\eta = 1.25$		$\eta = 1.75$	
	L_∞	CO	L_∞	CO
$\frac{1}{4}$	6.3121e-03	–	7.3108e-03	–
$\frac{1}{8}$	2.0741e-03	1.6054	2.1174e-03	1.7877
$\frac{1}{16}$	6.0017e-04	1.7890	6.0345e-04	1.8110
$\frac{1}{32}$	1.5674e-04	1.9370	1.7130e-04	1.8167

Example 4.3 We consider the space fractional tempered fractional diffusion-wave model under the interval $x \in [0, 1]$ and $t \in (0, 1]$ as

$$w_t(x, t) = \frac{1}{\Gamma(\mu - 1)} \int_0^t (t - \tau)^{\mu-2} e^{-\omega(t-\tau)} \mathbf{A}_x \frac{\partial^\eta w(x, y, \tau)}{\partial |x|^\eta} d\tau + g(x, t), \tag{4.1}$$

where $1 < \mu, \eta \leq 2$ with the initial and boundary conditions:

$$\begin{aligned} w(x, 0) &= 0, \quad x \in [0, 1], \\ w(x, t) &= 0, \quad x \in \partial([0, 1]), \quad t \in (0, 1). \end{aligned}$$

For the proposed problem, the exact solution is given by $w(x, t) = t^3 e^{-\omega t} (x(1-x))^2$ and this type of problem was studied in [16]. By putting the exact solution into (4.1), we can calculate the source term $g(x, t)$. We solve the proposed model using the presented scheme for different values of η when $\omega = 0.1$ and $\Delta t = 0.001$. Numerical results for this model using the presented method for various values of η when $\Delta t = 0.001$ are shown in Fig. 8. Figure 9 demonstrates the absolute error of the proposed method for various values of η when $\Delta t = 0.001$. In Table 6, we show a comparison between the numerical method presented in this paper and the numerical method studied in [16] based on the absolute error and computational orders. From the table and figures, we can see that the proposed method has better accuracy and performance.

5 Conclusion

The equation used in this article is the two-dimensional Riesz space distributed-order diffusion-wave equation, which is one of the most important and practical equations in mathematical and physical models. This work discussed a numerical method based on linear B-spline interpolation and the finite element method to solve the proposed equations. For the discretization of an integral part of the distribution order, the midpoint quadrature rule and linear B-spline interpolation have been used in the time direction. The Galerkin finite element method has been applied to discretize the Riemann-Liouville fractional integral in terms of the Riesz fractional operator. The convergence and stability analysis have been displayed using the energy method, and we demonstrated that the expanded numerical scheme has the convergence order $h^2 + (\Delta t)^2 + \vartheta^2$. In the end, two numerical examples have been given to show the efficiency of the proposed method. In the future, the proposed method can be implemented on several types of Riesz space distributed-order diffusion-wave equations as well as on different kinds of FDEs.

Author contributions The authors equally contributed to this work. All authors read and approved the final manuscript.

Funding There is no funding to declare for this research study.

Data Availability No data were used to support this study.

Declarations

Conflict of interest The authors declare that they have no competing interests.

References

1. A. Ansari, M.H. Derakhshan, H. Askari, Distributed order fractional diffusion equation with fractional Laplacian in axisymmetric cylindrical configuration. *Communications in Nonlinear Science and Numerical Simulation* **113**, 106590 (2022)
2. A. Ansari, M.H. Derakhshan, On spectral polar fractional Laplacian. *Mathematics and Computers in Simulation* **206**, 636–663 (2023)
3. A. Ansari, M.H. Derakhshan, Time-space fractional Euler-Poisson-Darboux equation with Bessel fractional derivative in infinite and finite domains. *Mathematics and Computers in Simulation* **218**, 383–402 (2024)
4. A. Ansari, Fundamental solution of a multi-dimensional distributed order fractional diffusion equation. *The European Physical Journal Plus* **136**(4), 1–23 (2021)
5. W. Bu, Y. Tang, Y. Wu, J. Yang, Finite difference/finite element method for two-dimensional space and time fractional Bloch-Torrey equations. *Journal of Computational Physics* **293**, 264–279 (2015)
6. A.H. Bhrawy, E.H. Doha, D. Baleanu, S.S. Ezz-Eldien, M.A. Abdelkawy, An accurate numerical technique for solving fractional optimal control problems. *Proceedings of the Romanian Academy Series A-Mathematics Physics Technical Sciences Information Science Impact Factor & Key. Scientometrics* **16**(1), 47–54 (2015)
7. W. Bu, A. Xiao, W. Zeng, Finite difference/finite element methods for distributed-order time fractional diffusion equations. *Journal of Scientific Computing* **72**(3), 422–441 (2017)
8. R.L. Bagley, P.J. Torvik, On the existence of the order domain and the solution of distributed order equations-Part II. *International Journal of Applied Mathematics* **2**(8), 965–988 (2000)
9. M. Chen, W. Deng, Discretized fractional substantial calculus ESAIM: *Mathematical Modelling and Numerical Analysis* **49**(2), 373–394 (2015)
10. M. Chen, W. Deng, A second-order accurate numerical method for the space-time tempered fractional diffusion-wave equation. *Applied Mathematics Letters* **68**, 87–93 (2017)
11. M. Caputo, Mean fractional-order-derivatives differential equations and filters. *Annali dell'Universita di Ferrara* **41**(1), 73–84 (1995)
12. A. Chakraborty, P. Veerasha, Effects of global warming, time delay and chaos control on the dynamics of a chaotic atmospheric propagation model within the frame of Caputo fractional operator. *Communications in Nonlinear Science and Numerical Simulation* **128**, 107657 (2024)
13. A. Chakraborty, P. Veerasha, A. Ciancio, H.M. Baskonus, M. Alsulami, The effect of climate change on the dynamics of a modified surface energy balance-mass balance model of Cryosphere under the frame of a non-local operator. *Results in Physics* **54**, 107031 (2023)
14. S. Deepika, P. Veerasha, Dynamics of chaotic waterwheel model with the asymmetric flow within the frame of Caputo fractional operator. *Chaos, Solitons & Fractals* **169**, 113298 (2023)
15. M. Dehghan, J. Manafian, A. Saadatmandi, Solving nonlinear fractional partial differential equations using the homotopy analysis method. *Numerical Methods for Partial Differential Equations* **26**(2), 448–479 (2010)
16. M. Dehghan, M. Abbaszadeh, A finite difference/finite element technique with error estimate for space fractional tempered diffusion-wave equation. *Computers & Mathematics with Applications* **75**(8), 2903–2914 (2018)
17. W. Ding, S. Patnaik, S. Sidhardh, F. Semperlotti, Applications of distributed-order fractional operators: A review. *Entropy* **23**(1), 110 (2021)
18. V.J. Ervin, J.P. Roop, Variational formulation for the stationary fractional advection dispersion equation. *Numerical Methods for Partial Differential Equations* **22**, 558–576 (2006)
19. R. Gorenflo, F. Mainardi, Random walk models for space-fractional diffusion processes. *Fractional Calculus and Applied. Analysis* **1**, 167–191 (1998)
20. R. Gorenflo, Y. Luchko, M. Stojanović, Fundamental solution of a distributed order time-fractional diffusion-wave equation as probability density. *Fractional Calculus and Applied Analysis* **16**(2), 297–316 (2013)
21. G.H. Gao, Z.Z. Sun, Two difference schemes for solving the one-dimensional time distributed-order fractional wave equations. *Numerical Algorithms* **74**, 675–697 (2017)
22. T. Guo, O. Nikan, Z. Avazzadeh, W. Qiu, Efficient alternating direction implicit numerical approaches for multi-dimensional distributed-order fractional integro differential problems. *Computational and Applied Mathematics* **41**(6), 236 (2022)
23. R. Hilfer, *Applications of Fractional Calculus in Physics* (World Scientific, Singapore, 2000)
24. M.H. Heydari, M. Razzaghi, D. Baleanu, A numerical method based on the piecewise Jacobi functions for distributed-order fractional Schrödinger equation. *Communications in Nonlinear Science and Numerical Simulation* **116**, 106873 (2023)
25. C. Huang, H. Chen, N. An, β -robust super-convergent analysis of a finite element method for the distributed order time-fractional diffusion equation. *Journal of Scientific Computing* **90**(1), 44 (2022)
26. J. Hristov, Linear viscoelastic responses and constitutive equations in terms of fractional operators with non-singular kernels-pragmatic approach, memory kernel correspondence requirement and analyses. *The European Physical Journal Plus* **134**(6), 283 (2019)
27. E. Ilhan, P. Veerasha, H.M. Baskonus, Fractional approach for a mathematical model of atmospheric dynamics of CO₂ gas with an efficient method. *Chaos, Solitons & Fractals* **152**, 111347 (2021)
28. J. Korbel, Y. Luchko, Modeling of financial processes with a space-time fractional diffusion equation of varying order. *Fractional Calculus and Applied Analysis* **19**(6), 1414–1433 (2016)
29. M. Khater, Analytical and numerical-simulation studies on a combined mKdV-KdV system in the plasma and solid physics. *The European Physical Journal Plus* **137**(9), 1–9 (2022)
30. P. Kumar, V.S. Erturk, M. Murillo-Arcila, V. Govindaraj, A new form of L1-Predictor-Corrector scheme to solve multiple delay-type fractional order systems with the example of a neural network model. *Fractals* (2023)
31. Z. Li, Y. Luchko, M. Yamamoto, Analyticity of solutions to a distributed order time-fractional diffusion equation and its application to an inverse problem. *Computers & Mathematics with Applications* **73**, 1041–1052 (2016)
32. M. Li, C. Huang, F. Jiang, Galerkin finite element method for higher dimensional multi-term fractional diffusion equation on non-uniform meshes. *Applicable Analysis* **96**(8), 1269–1284 (2017)
33. C.F. Lorenzo, T.T. Hartley, Variable order and distributed order fractional operators. *Nonlinear dynamics* **29**, 57–98 (2002)
34. S. Mashayekhi, M. Razzaghi, Numerical solution of distributed order fractional differential equations by hybrid functions. *Journal of Computational Physics* **315**, 169–181 (2016)

35. H.R. Marasi, M.H. Derakhshan, A.A. Ghuraibawi, P. Kumar, A novel method based on fractional order Gegenbauer wavelet operational matrix for the solutions of the multi-term time-fractional telegraph equation of distributed order. *Mathematics and Computers in Simulation* **217**, 405–424 (2024)
36. H. Marasi, M.H. Derakhshan, A composite collocation method based on the fractional Chelyshkov wavelets for distributed-order fractional mobile-immobile advection-dispersion equation. *Mathematical Modelling and Analysis* **27**(4), 590–609 (2022)
37. Y. Mahatekar, P.S. Scindia, P. Kumar, A new numerical method to solve fractional differential equations in terms of Caputo-Fabrizio derivatives. *Physica Scripta* **98**(2), 024001 (2023)
38. M.K. Naik, C. Baishya, P. Veerasha, D. Baleanu, Design of a fractional-order atmospheric model via a class of ACT-like chaotic system and its sliding mode chaos control *Chaos: An Interdisciplinary Journal of Nonlinear Science* **33**(2), 023129 (2023)
39. Y. Niu, Y. Liu, H. Li, F. Liu, Fast high-order compact difference scheme for the nonlinear distributed-order fractional Sobolev model appearing in porous media. *Mathematics and Computers in Simulation* **203**, 387–407 (2023)
40. K.B. Oldham, J. Spanier, *The Fractional Calculus*, Academic Press (1974)
41. Z. Odibat, V.S. Erturk, P. Kumar, V. Govindaraj, Dynamics of generalized Caputo type delay fractional differential equations using a modified Predictor-Corrector scheme. *Physica Scripta* **96**(12), 125213 (2021)
42. I. Podlubny, *Fractional Differential Equations*, Academic Press (1999)
43. M. Pournabae, A. Saadatmandi, A new operational matrix based on Müntz-Legendre polynomials for solving distributed order fractional differential equations. *Mathematics and Computers in Simulation* **194**, 210–235 (2022)
44. A. Patra, An effective comparison involving a novel spectral approach and finite difference method for the Schrödinger equation involving the Riesz fractional derivative in the quantum field theory. *The European Physical Journal Plus* **133**, 1–14 (2018)
45. A. Quarteroni, A. Valli, *Numerical Approximation of Partial Differential Equations* (Springer-Verlag, New York, 1997)
46. W. Qiu, D. Xu, H. Chen, J. Guo, An alternating direction implicit Galerkin finite element method for the distributed-order time-fractional mobile-immobile equation in two dimensions. *Computers & Mathematics with Applications* **80**(12), 3156–3172 (2020)
47. H. Ye, F. Liu, V. Anh, Compact difference scheme for distributed-order time-fractional diffusion-wave equation on bounded domains. *Journal of Computational Physics* **298**, 652–660 (2015)
48. H. Ye, F. Liu, V. Anh, I. Turner, Numerical analysis for the time distributed-order and Riesz space fractional diffusions on bounded domains. *IMA Journal of Applied Mathematics* **80**(3), 825–838 (2015)
49. Z. Wang, S. Vong, Compact difference schemes for the modified anomalous fractional sub-diffusion equation and the fractional diffusion-wave equation. *J. Comput. Phys.* **277**, 1–15 (2014)

Springer Nature or its licensor (e.g. a society or other partner) holds exclusive rights to this article under a publishing agreement with the author(s) or other rightsholder(s); author self-archiving of the accepted manuscript version of this article is solely governed by the terms of such publishing agreement and applicable law.